Biophysical Chemistry 159 (2011) 194–204

Contents lists available at ScienceDirect

Biophysical Chemistry

journal homepage: http://www.elsevier.com/locate/biophyschem

The soluble, periplasmic domain of OmpA folds as an independent unit and displays chaperone activity by reducing the self-association propensity of the unfolded OmpA transmembrane β-barrel

Emily J. Danoff, Karen G. Fleming *

T. C. Jenkins Department of Biophysics, Johns Hopkins University, 3400 North Charles Street, Baltimore, MD 21218, USA

ARTICLE INFO

Article history:
Received 1 April 2011
Received in revised form 13 June 2011
Accepted 20 June 2011
Available online 6 July 2011

Keywords:
Membrane protein
Protein folding
Circular dichroism
Sedimentation velocity

ABSTRACT

OmpA is one of only a few transmembrane proteins whose folding and stability have been investigated in detail. However, only half of the OmpA mass encodes its transmembrane β-barrel; the remaining sequence is a soluble domain that is localized to the periplasmic side of the outer membrane. To understand how the OmpA periplasmic domain contributes to the stability and folding of the full-length OmpA protein, we cloned, expressed, purified and studied the OmpA periplasmic domain independently of the OmpA transmembrane β-barrel region. Our experiments showed that the OmpA periplasmic domain exists as an independent folding unit with a free energy of folding equal to -6.2 (± 0.1) kcal mol^{-1} at 25 °C. Using circular dichroism, we determined that the OmpA periplasmic domain adopts a mixed alpha/beta secondary structure, a conformation that has previously been used to describe the partially folded non-native state of the full-length OmpA. We further discovered that the OmpA periplasmic domain reduces the self-association propensity of the unfolded barrel domain, but only when covalently attached (in cis). *In vitro* folding experiments showed that self-association competes with β-barrel folding when allowed to occur before the addition of membranes, and the periplasmic domain enhances the folding efficiency of the full-length protein by reducing its self-association. These results identify a novel chaperone function for the periplasmic domain of OmpA that may be relevant for folding *in vivo*. We have also extensively investigated the properties of the self-association reaction of unfolded OmpA and found that the transmembrane region must form a critical nucleus comprised of three molecules before undergoing further oligomerization to form large molecular weight species. Finally, we studied the conformation of the unfolded OmpA monomer and found that the folding-competent form of the transmembrane region adopts an expanded conformation, which is in contrast to previous studies that have suggested a collapsed unfolded state.

1. Introduction

Over the past two decades, the transmembrane protein OmpA has been extensively investigated as a model for membrane protein folding. OmpA folds into a large number of hydrophobic environments, including many different detergents and lipid compositions [1–8]. A folding pathway describing the conformational changes and kinetic phases that OmpA must undergo to attain its native conformation in membranes was proposed in the late 1990s [4], and OmpA is one of only three transmembrane proteins whose thermodynamic stability has been measured in phospholipid vesicles [9].

However, examination of the sequence shows that the full-length OmpA is actually a two-domain protein in which only the N-terminal half ($OmpA_{171}$, residues 1–171) is a membrane-embedded β-barrel [10]. In contrast, the remaining sequence of OmpA (172–325) comprises a soluble, periplasmic domain ($OmpA_{Per}$). The contributions of $OmpA_{Per}$ to the kinetic pathways and thermodynamic stability of the full-length OmpA protein ($OmpA_{325}$) have not been explicitly investigated and have, in fact, largely been ignored. One reason for this is that changes in the conformation of the periplasmic domain are mostly invisible to the methods that have been employed in studying OmpA folding [1–4,6,8,9,11–13]. Many folding investigations of OmpA use tryptophan fluorescence spectroscopy as a reporter of changes to the protein's conformation and/or environment; however, all five of the OmpA tryptophan residues are located in the transmembrane β-barrel region (see Fig. 1A and B), while none are located in the periplasmic sequence. Therefore fluorescence studies would not detect changes in the conformation of the periplasmic domain. The other principal method used to measure OmpA folding takes advantage of the fact that microbial β-barrel proteins show a different migration on SDS-PAGE gels depending on whether they are folded or unfolded [14]. Since the periplasmic domain is soluble, it does not show this behavior, so changes to its conformation would not be detected by this assay either.

This manuscript is a contribution to a special issue commemorating the 25th annual meeting of the Gibbs Society of Biothermodynamics.

* Corresponding author. Tel.: +1 410 516 7256; fax: +1 410 516 4118.
E-mail address: Karen.Fleming@jhu.edu (K.G. Fleming).

0301-4622/$ – see front matter © 2011 Elsevier B.V. All rights reserved.
doi:10.1016/j.bpc.2011.06.013

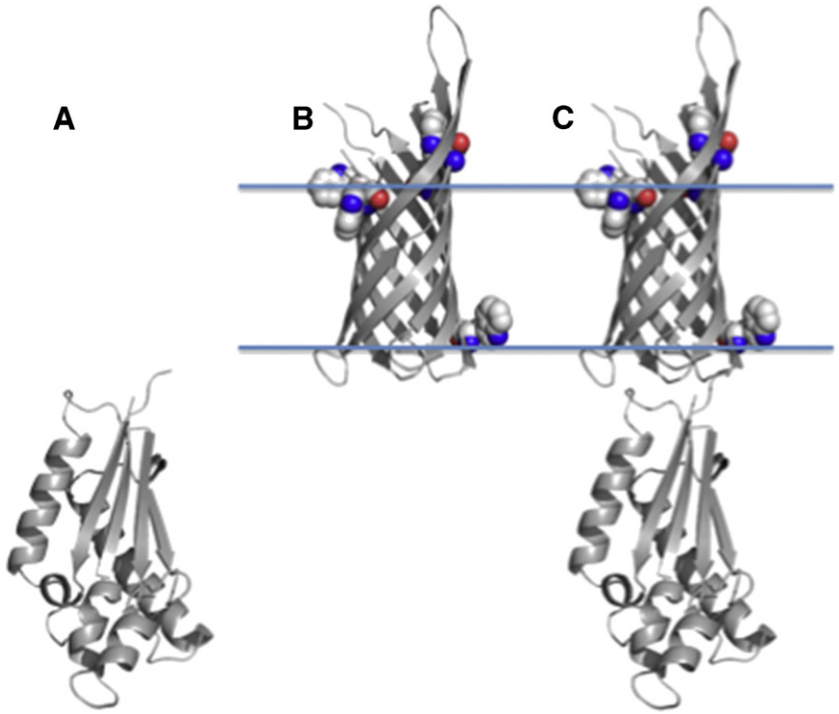

Fig. 1. Structural models of the proteins used in this study. (A) Homology model of $OmpA_{Per}$. (B) Crystal structure of $OmpA_{171}$ (PDB id 1QJP). (C) Model of full-length OmpA ($OmpA_{325}$) created by combining the structures of $OmpA_{Per}$ and $OmpA_{171}$. The relative orientations are unknown and arbitrarily placed. The Tryptophan residues in the transmembrane β-barrel region are shown as spheres. All figures were created using Pymol.

In keeping with the Gibbs tradition of dissecting a system into its components and examining the individual contributions of each part to overall biological function, we examine the structural features and thermodynamic stability of the OmpA periplasmic domain in isolation, as well as its interactions and role in folding with regard to the β-barrel domain of OmpA. We use circular dichroism spectroscopy, sedimentation velocity, and *in vitro* folding to study the conformation and interactions of the individual domains of OmpA in the context of the behavior of the full-length protein. Our studies significantly revise previous ideas about the unfolded state conformations and interactions of OmpA and contribute to a more complete and accurate scheme for its kinetic folding pathway. In addition, we discover a novel chaperone function of the periplasmic domain that may be relevant for OmpA folding *in vivo*.

2. Materials and methods

2.1. Construction of the $OmpA_{Per}$ homology model

We submitted the amino acid sequence corresponding to the OmpA periplasmic domain to the Swiss-Model web server (http://swissmodel.expasy.org/). This server used the *Neisseria meningitis* RmpM OmpA-like domain structure (1R1M) solved by Grizot and Buchanan [15] as a best match to template a homology model of the *E. coli* OmpA periplasmic domain. These two sequences share 37.1% sequence identity, which is higher than the 30% threshold sequence identity needed for accurate model building, and the resultant model of the OmpA periplasmic domain is essentially superimposable upon the 1R1M structure with the exception of one loop region in which 1R1M has an extra turn of helix both preceding and following one turn (Supplementary Fig. 1).

2.2. Cloning and expression of proteins

The mature form of full-length OmpA ($OmpA_{325}$) and the N-terminal barrel domain ($OmpA_{171}$) were PCR amplified using primers designed to include NdeI (5′) and BamHI (3′) sites (primers are listed in Supplemental Table 1). The OmpA constructs were amplified using ExTaq polymerase (Takara) from an overnight growth of *E. coli* K12 MG1655. The PCR products were ligated into the pCR2.1-TOPO vector using a TOPO TA cloning kit (Invitrogen). QuikChange site-directed mutagenesis (Stratagene) was used to remove an internal BamHI site in $OmpA_{325}$, which did not change the amino acid sequence. The plasmids were restricted with NdeI and BamHI, and the insert was ligated into a pET11a vector. These plasmids were transformed into DH5α cells, and the sequences were confirmed by double-stranded DNA sequencing.

The periplasmic domain of OmpA ($OmpA_{Per}$) was PCR amplified using primers incorporating NdeI (5′) and XhoI (3′) sites. The gene was amplified from the $OmpA_{325}$ gene in pET11a and ligated into the TOPO vector. The plasmid was cut with restriction enzymes and ligated into a pET28b vector, which expresses the protein with an N-terminal His-tag followed by a TEV cleavage site. The plasmid was transformed into DH5α and the sequence was confirmed by DNA sequencing.

Plasmids for the three OmpA constructs were separately transformed into hms174(DE3) cells and grown in 500 ml of TB medium at 37 °C with shaking to an optical density of 0.8 at 600 nm. Protein expression was induced by the addition of 1 mM IPTG and cells were incubated for 4–6 h at 37 °C with shaking before harvesting by centrifugation (5000 rpm, 15 minutes, 4 °C). Cell pellets were frozen for periods of time ranging from overnight to several days before undergoing further processing.

2.3. Preparation of urea solutions

Ultra-pure urea was purchased from Amresco. Urea solutions were prepared at a concentration of 10 M in water and deionized by adding AG 501-X8 resin (BioRad) at a ratio of 1 g resin for every 20 ml of solution. Solutions were stirred with the resin for 1 h at room temperature. The resin was removed by filtration and the urea used to prepare Urea Buffer (8 M urea, 20 mM Tris, pH 8). The final urea concentration was determined by refractometry. For purifications

of $OmpA_{325}$, Urea Buffer contained 2 mM TCEP (Pierce). Urea Buffer was stored at −20 °C.

2.4. Purification of $OmpA_{325}$ and $OmpA_{171}$

A pellet from a 500 ml growth was resuspended in 25 ml of Lysis Buffer (50 mM Tris, pH 8, 40 mM EDTA) and lysed by French press. Brij-35 (Sigma) was added to a final concentration of 0.1%, and inclusion bodies were isolated by centrifugation at 5500 rpm for 30 minutes. These were washed twice by resuspension in 25 ml of Wash Buffer (10 mM Tris, pH 8, 1 mM EDTA) followed by pelleting by centrifugation under the same conditions. Purified inclusion bodies were resuspended a third time in Wash Buffer and split into four fractions before a final centrifugation. The supernatant was discarded and inclusion body pellets were stored at −20 °C.

An inclusion body pellet was dissolved in 7 ml of Urea Buffer and clarified by centrifugation. The supernatant was filtered through a 0.45 μm pore (Millipore). Protein samples were further purified using a BioRad BioLogic DuoFlow Chromatography System. Samples were loaded onto an UNO Q6 continuous bed anion exchange column (BioRad) and eluted with a NaCl gradient in Urea Buffer. Protein-containing fractions were pooled and concentrated using centrifugal filtration (Millipore). Samples were de-salted and further purified using a Superdex 200 10/300 GL gel filtration column (GE Healthcare), run in Urea Buffer. Protein-containing fractions were pooled and concentrated as before. Protein concentration was determined by measuring the absorbance at 280 nm and using extinction coefficients calculated in Sednterp [16]. These values are reported in Supplemental Table 2. Purified unfolded $OmpA_{325}$ and $OmpA_{171}$ were aliquoted into Eppendorf tubes and stored at −80 °C until use.

2.5. Purification of $OmpA_{Per}$

A pellet from a 500 ml growth was resuspended in 25 ml of Buffer A (20 mM sodium phosphate, pH 8, 500 mM NaCl, 20 mM imidazole) and a tablet of complete EDTA-free protease inhibitor cocktail (Roche) added. Cells were lysed by French press and the lysate clarified by centrifugation at 5500 rpm for 30 minutes. The supernatant was retained and DNase (Roche) added to a final concentration of 2 μg ml^{-1}. The sample was filtered through a 0.45 μm pore (Millipore). His-tagged $OmpA_{Per}$ was purified by loading the sample on a column packed with Ni Sepharose High Performance (GE Healthcare) and eluting with Buffer B (20 mM Sodium Phosphate, pH 8, 500 mM NaCl, 500 mM imidazole). The His-tag was removed by incubation overnight with TEV protease [17] (1:20 molar ratio TEV: $OmpA_{Per}$) and the sample dialyzed into Buffer A. Cleaved protein was isolated by passing the sample through the Ni column again. Protein-containing fractions were pooled and dialyzed into 20 mM Tris, pH 8. The concentration was determined using the extinction coefficient listed in Supplemental Table 2. $OmpA_{Per}$ was stored at 4 °C until use.

2.6. Vesicle preparation

1,2-Didecanoyl-*sn*-Glycero-3-Phosphocholine ($diC_{10}PC$) lipids dissolved in chloroform (Avanti Polar Lipids) were dried to a thin film in glass vials under a gentle stream of nitrogen gas. The lipid films were evacuated overnight to remove residual solvent and stored at −20 °C until use. For vesicle preparation, lipid films were reconstituted in 20 mM Tris, pH 8 at a concentration of 10 mg ml^{-1} and large unilamellar vesicles (LUVs) were made by extruding reconstituted lipids 21 times though a 0.1 μm filter using a mini-extruder (Avanti).

2.7. Circular dichroism

CD measurements were performed using an Aviv circular dichroism Spectrometer, Model 410 (Aviv Biomedical), with a custom inset detector to reduce light scattering. Wavelength spectra were recorded at 25 °C between 200 and 280 nm in 1 nm increments, with an averaging time of 5 s. For each sample, three scans were recorded and averaged. A path length of 1 cm or 1 mm was used (Hellma cuvettes) and spectra of empty cuvettes were subtracted from sample spectra to correct for background signal. For samples containing LUVs, spectra of LUV-only mixtures were used for background subtraction.

Thermodynamic measurements on $OmpA_{Per}$ were performed using an automated Hamilton Dispenser, MICROLAB 540B. In unfolding titrations, an appropriate amount of Urea Buffer was titrated into a folded sample followed by incubation at 25 °C while stirring for 1 minute before taking a measurement. The CD signal was monitored at 220 nm with an averaging time of 5 s. Measurements were corrected for protein dilution. Refolding titrations were performed in a similar manner, with the titrator dispensing buffer instead of denaturant, and the initial sample prepared in 7.5 M urea. Titration data were fit using the linear extrapolation method of Santoro and Bolen [18,19].

2.8. CD kinetics

CD signal kinetics were measured for $OmpA_{325}$ and $OmpA_{171}$ at various concentrations and in 600 mM urea, 20 mM Tris, pH 8. The CD signal was monitored at 218 nm for approximately 16 hours, with the sample incubated at 25 °C and without stirring. The interval between data points was 60 s and the time constant was 10 s. The CD signal was converted to fraction monomer using the values measured for completely monomeric protein and completely self-associated protein.

The method of initial rates was used to estimate the order of the self-association reaction [8]. For the general reaction,

$$A \rightarrow B$$

the rate of reaction is given by the following expression:

$$-\frac{d[A](t)}{dt} = k[A]^n(t) \tag{1}$$

where k is the rate constant and n is the order of the reaction. At early timepoints, the concentration of A can be approximated as the starting concentration, $[A]_o$, so the initial rate of reaction can be expressed as:

$$-\left(\frac{d[A]}{dt}\right)_{t=0} = k[A]_o^n \tag{2}$$

A double logarithmic plot of the initial rate as a function of $[A]_o$ is linear and has a slope of n, the order of the reaction:

$$\ln\left(-\left(\frac{d[A]}{dt}\right)_{t=0}\right) = n\ln([A]_o) + \ln k \tag{3}$$

To determine the order of the OmpA self-association reaction, the CD kinetics were plotted as monomer concentration *versus* time and a line fit to the earliest time points. The slopes were plotted on a double logarithmic plot as a function of total OmpA concentration, and a line was fitted to the data.

The kinetics data were further analyzed using a nucleated growth polymerization model [20] in order to determine the critical nucleus size, n^*. According to this model, at early time points the concentration of monomer units incorporated into polymers (Δ) varies linearly with time squared [20]:

$$\Delta(t) = s(c)t^2 \tag{4}$$

where $s(c)$ is the slope of this line and is a function of total monomer concentration, c, and the critical nucleus, n^*:

$$s(c) \propto c^{n^* + 2} \quad (5)$$

A double logarithmic plot of s as a function of total monomer concentration, c, is linear and has a slope of $n^* + 2$.

To perform this analysis on the CD kinetics data, the data were transformed to plot associated OmpA *versus* time squared and a line fit to the earliest time points. The slopes were plotted on a double logarithmic plot as a function of total OmpA concentration, and a line was fitted to the data.

2.9. Sedimentation velocity analytical ultracentrifugation

Sedimentation velocity experiments were carried out in a Beckman XL-A analytical ultracentrifuge, using two-sector cells and an An60Ti rotor. All experiments were carried out at a speed of 50,000 rpm and 25 °C. All sedimentation profiles were detected using absorbance optics operated in continuous mode. Protein molecular weights, partial specific volumes, extinction coefficients and buffer densities were calculated using Sednterp [16].

2.10. Sedimentation velocity: self-association of unfolded $OmpA_{325}$ and $OmpA_{171}$

To study the concentration dependence of OmpA self-association, samples were prepared at varying protein concentrations in 20 mM Tris, pH 8 and various urea concentrations. $OmpA_{325}$ samples also contained 2 mM TCEP, in order to eliminate disulfide-bond mediated dimer formation (this was unecessary for $OmpA_{171}$ since the two cysteine residues responsible for disulfide bonding are located in the periplasmic domain). After dilution of the protein from high urea to the final condition, the samples were loaded into the sedimentation velocity cells, placed in the rotor and temperature equilibrated prior to rotor acceleration. To ensure consistency, the total time for these steps was controlled so that the rotor would start 30 minutes after protein dilution. Sedimentation velocity profiles were detected using the absorbance optics at a single wavelength adjusted between 227 nm and 235 nm to obtain an absorbance signal between 0.1 and 1.3.

When analyzing the sedimentation data, the scans were divided into two analysis windows based on the apparent populated species: either monomer (late scans) or oligomer (early scans). However, care was taken to examine all scans for the presence of intermediate sedimentation coefficients. Sedimentation coefficient distribution peaks obtained in DCDT+ at low s-values were fitted to Gaussian equations to confirm they contained monomeric protein, and the concentration of monomer was determined by integrating the area under the monomeric $g(s^*)$ peak. Very broad distributions were observed at large s-values, and the entire oligomeric peak was integrated to determine the concentration of these species. The fraction monomer was calculated as the concentration of monomer divided by the sum of monomer and oligomers. Data were also analyzed by the $c(s^*)$ method as implemented in SedFit [21] and the fraction monomer found by integration of the $c(s^*)$ curve agreed well with that found by $g(s^*)$.

2.11. Sedimentation velocity: time-dependence of self-association

To determine the kinetics of OmpA self-association, samples were prepared as above, and incubated for various times before initiating centrifugation. Data were analyzed as described above to determine the fraction monomer at each timepoint.

2.12. Sedimentation velocity: hydrodynamic shape estimates

The urea dependence of the hydrodynamic shape of unfolded $OmpA_{325}$ and $OmpA_{171}$ was analyzed by sedimentation velocity of samples at a concentration of 2 μM in various urea concentrations. Sedimentation velocity data were analyzed using the time derivative method of Stafford as implemented in DCDT+ [22]. The monomer peaks in the $g(s^*)$ curves were fit for molecular weight and sedimentation coefficient. After converting to $s^*_{20,w}$, the s-values were plotted as a function of urea, and a linear extrapolation was used to determine the sedimentation coefficient in the absence of urea. Perrin's equations as implemented in Sednterp were used to calculate the axial ratio of a prolate ellipsoid of revolution for the species.

2.13. Delayed folding experiments

$OmpA_{325}$ or $OmpA_{171}$ were diluted into a folding condition that lacked vesicles (2 μM or 5 μM protein, 600 mM urea) and incubated at 25 °C for 30 minutes before the addition of LUVs at a final lipid to protein ratio of 800:1, to initiate folding. Samples underwent gentle stirring during folding. Certain folding mixtures also contained equimolar concentrations of $OmpA_{Per}$ (2 μM or 5 μM). Folding reactions were quenched after 3 h by the addition of 5× SDS gel-loading buffer to a final concentration of 1×. The fraction folded was determined by SDS-PAGE using acrylamide precast gels from BioRad, staining with Coomassie blue, and digital transmission scanning (Epson 4490). Densitometry was performed using the freely available ImageJ software, and the fraction folded was calculated by dividing the intensity of the folded band by the sum of the intensities of the folded and unfolded bands.

3. Results

3.1. The OmpA periplasmic domain adopts a mixed alpha/beta secondary structure that can fold independently of the transmembrane region

Nearly 20 years ago, Surrey and Jähnig showed that OmpA adopted a mixed alpha/beta secondary structure immediately upon dilution to a folding condition (<100 mM urea) from high (>6 M) urea concentrations [4]. This form has been referred to in the literature as a "partially folded" state from which folding begins in aqueous solutions with vesicles. However, it has always been unclear whether this secondary structure arises from conformations of the periplasmic domain, the transmembrane β-barrel domain, or both. This ambiguity is essential to resolve because elucidation of physically based folding schemes requires knowing the set of conformations that polypeptide sequences can sample along a folding trajectory.

Since the mixed alpha/beta secondary structure arose immediately upon dilution of OmpA to a folding condition, we hypothesized that this secondary structure might represent the folding of the OmpA periplasmic domain rather than a non-native conformation adopted by the transmembrane β-barrel region. We began to address this question by constructing a homology model for $OmpA_{Per}$ to determine whether such a structural model would even be consistent with the CD data. Shown in Fig. 1A, this model is indeed well described as mixed alpha/beta secondary structure.

$OmpA_{171}$ had previously been shown to independently adopt the transmembrane β-barrel fold; its structure is shown in Fig. 1B [10]. Fig. 1C shows the two domains combined together at the same scale in Pymol in a representation of the full-length OmpA ($OmpA_{325}$).

To determine whether the observed mixed alpha/beta structure of full-length OmpA was due to the periplasmic domain, the β-barrel domain, or both, we cloned, expressed and purified $OmpA_{Per}$, $OmpA_{171}$, and $OmpA_{325}$ independently of each other and measured the CD spectra of the three constructs. Fig. 2A shows CD spectra of $OmpA_{Per}$ alone, folded in aqueous Tris buffer (solid blue) and unfolded

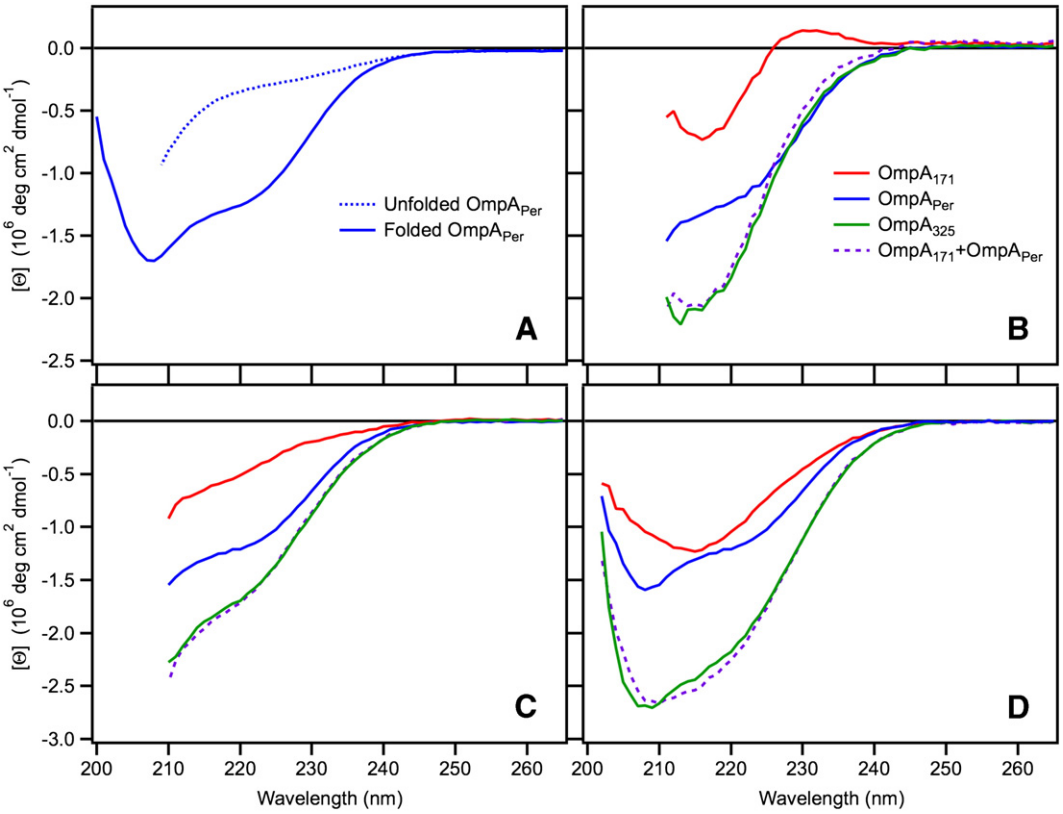

Fig. 2. CD wavelength spectra of OmpA constructs. All spectra were measured at 25 °C and are plotted as molar ellipticity. (A) $OmpA_{Per}$ under folding (solid blue) and unfolding (dotted blue) conditions. Folded $OmpA_{Per}$ was measured at a concentration of 40 μM in 20 mM Tris, pH 8, with a 1 mm pathlength. Unfolded $OmpA_{Per}$ was measured at a concentration of 20 μM in 6.1 M urea, 20 mM Tris, pH 8, with a 1 mm pathlength. (B) Spectra of folded proteins: $OmpA_{171}$ (red), $OmpA_{Per}$ (blue), and $OmpA_{325}$ (green) were incubated in β-barrel folding conditions for 6 h (1 μM protein, 800 μM $diC_{10}PC$ LUVs, 600 mM urea, 20 mM Tris, pH 8, 25 °C). Data were collected with a 1 cm pathlength. The spectrum for an LUV-only sample was used for background subtraction. The mathematical sum of $OmpA_{171}$ and $OmpA_{Per}$ is shown as a purple dashed line. (C) and (D) Spectra for unfolded $OmpA_{171}$ and folded $OmpA_{Per}$. In (C) protein samples were prepared at 1 μM in 600 mM urea, 20 mM Tris, pH 8 (monomer conditions) and measured with a 1 cm pathlength. In (D) protein samples were 10 μM in 600 mM urea, 20 mM Tris, pH 8 (self-associating conditions) and were allowed to incubate at room temperature overnight before measurements were made with a 1 mm pathlength. Curves are colored as in (B).

in 6 M urea (dotted blue). It is apparent from these spectra that folded $OmpA_{Per}$ has mixed alpha/beta structure, as indicated by the double trough at 208 and 222 nm. In 6 M urea the protein has no regular structure, consistent with an unfolded conformation.

Panels B–D show CD data for $OmpA_{171}$ (red), $OmpA_{Per}$ (blue), and $OmpA_{325}$ (green) under various buffer conditions (described below) used to investigate the conformations of the two domains. The mathematical sum of the spectra for $OmpA_{171}$ and $OmpA_{Per}$ is shown as a dashed purple line in each panel. The data in all cases demonstrate that the mixed alpha/beta secondary structure characteristic of aqueous $OmpA_{325}$ arises entirely from $OmpA_{Per}$, even though the conformation of the $OmpA_{171}$ barrel region is dependent on the conditions employed.

Fig. 2B shows spectra collected at protein concentrations of 1 μM in 20 mM Tris, pH 8, 600 mM urea and $diC_{10}PC$ LUVs at a lipid to protein ratio of 800:1. In order to obtain a measurable signal from such a low protein concentration, a 1 cm path length was used and reliable data could only be collected above 210 nm. However, a distinctive β-trough at 216 nm can be observed for $OmpA_{171}$ (red), indicating that the barrel folds in the presence of LUVs. In addition, the 222 nm trough indicative of alpha-helix is present in the $OmpA_{Per}$ spectrum (blue), indicating that it is folded in the presence of 600 mM urea (this result is also consistent with the unfolding titration described below and shown in Fig. 3). The CD spectrum for full-length $OmpA_{325}$ (green) overlays well with the mathematical sum (dashed purple) of the spectra for $OmpA_{171}$ and $OmpA_{Per}$, indicating that these are independently folding domains. Interestingly, the spectrum of $OmpA_{171}$ reveals a novel 231 nm positive peak that we only observe under conditions where the β-barrel is folded. This peak has been previously observed in the PagP transmembrane β-barrel and has been attributed to a Cotton effect between aromatic groups that only forms when the PagP β-barrel is folded [23]. This positive peak

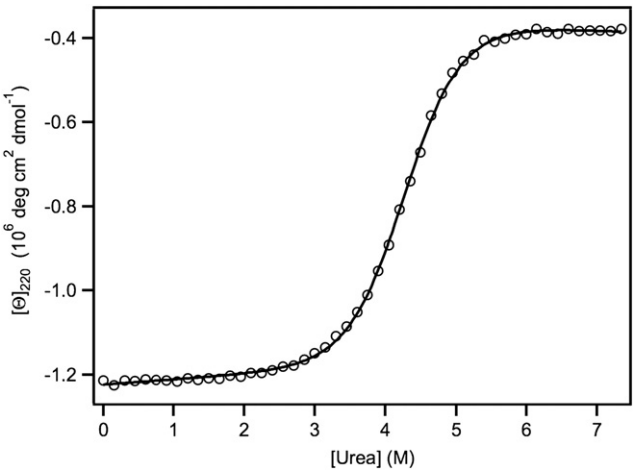

Fig. 3. Unfolding titration of $OmpA_{Per}$ measured by CD. Folded $OmpA_{Per}$ at a starting concentration of 8 μM in 20 mM Tris, pH 8 was titrated with 8 M urea in sequential steps. The CD signal was monitored at 220 nm and corrected for protein dilution. The data (open circles) were fit to a two-state model of unfolding (black line) and the linear extrapolation method used to determine the energy for folding in the absence of denaturant. Four titrations were performed and gave an average ΔG_F^0 equal to −6.2 (±0.1) kcal mol^{-1} with an m-value of −1.44 (±0.04) kcal mol^{-1} M $urea^{-1}$.

is masked in $OmpA_{325}$ by the negative α-helix signal arising from $OmpA_{Per}$.

Fig. 2C shows spectra for these three constructs in the same buffer conditions as 2B, except lacking LUVs (1 μM protein, 20 mM Tris, pH 8, 600 mM urea). As expected, the periplasmic domain (blue) does not require vesicles for folding and is folded under these conditions as confirmed by the alpha-helix trough deflection at 222 nm. However, $OmpA_{171}$ (red) displays a CD spectrum containing no regular structure, and it lacks the 231 nm positive peak, showing it is unfolded in the absence of vesicles. The mathematical sum (dashed purple) of these two spectra overlays upon that of full-length $OmpA_{325}$ (green). Altogether, these data show that the "folding competent" unfolded state of the OmpA transmembrane β-barrel region is not mixed alpha/beta, but rather contains no regular structure.

Fig. 2D shows the same buffer conditions as 2C (20 mM Tris, pH 8, 600 mM urea, no LUVs), except the protein concentration is higher (10 μM) and the samples have been allowed to incubate overnight. To accommodate this higher protein concentration, a 1 mm path length was used and data were collected down to 202 nm. We show below that 10 μM protein in 600 mM urea is a condition that results in self-association of the $OmpA_{325}$ and $OmpA_{171}$ unfolded states to form high molecular weight oligomers. However, even in this oligomeric form, the CD spectra of the two independent domains ($OmpA_{171}$ in red and $OmpA_{Per}$ in blue) sum to that of the full-length spectrum (green), indicating that self-association of OmpA unfolded states does not involve unfolding of its periplasmic domain. Interestingly, the CD spectra for self-associated $OmpA_{171}$ and $OmpA_{325}$ show very broad negative peaks in the beta region of the CD spectrum, but are distinctly different from the spectra of natively folded OmpA barrel in 2B. It is possible that this self-associated state contains non-native beta-structure, but further experimentation is needed to better characterize the conformation of this state.

As implied by the CD spectra, we expected that $OmpA_{Per}$ represented an independent folding domain. To demonstrate this, we determined its thermodynamic stability using chemical denaturation experiments. Folding of $OmpA_{Per}$ has been invisible in previous denaturation studies of OmpA because those studies used fluorescence spectroscopy or SDS-PAGE to measure folded and unfolded populations, and changes to the conformation of the periplasmic domain are not detected by these methods [9]. Fig. 3 shows a typical urea denaturation curve for $OmpA_{Per}$ measured using CD spectroscopy. The data are well described by two-state linear extrapolation equations [18,19] and reveal a free energy of folding in the absence of denaturant equal to -6.2 (± 0.1) kcal mol^{-1} with an m value of -1.44 (± 0.04) kcal mol^{-1} M $urea^{-1}$. The same values were obtained from measurements on protein from a completely separate purification. A refolding titration was also performed to verify the path independence of this measurement (data not shown).

3.2. The OmpA periplasmic domain acts in cis to reduce self-association of its unfolded β-barrel domain

In 1992, Surrey and Jähnig showed that the aqueous, unfolded state (U_{AQ}) of OmpA can slowly self-associate to form large oligomers [13]. Since OmpA presumably folds as a monomeric entity, the interactions of OmpA unfolded states would be detrimental to folding and should be a reaction that the cell would endeavor to control with chaperones. Moreover, the presence of oligomeric unfolded states represents an additional kinetic phase that must be considered in the development of folding pathways *in vitro*. Surrey and Jähnig formed the U_{AQ} state by diluting OmpA from high to low concentrations of urea in solutions that lacked vesicles (i.e. buffer conditions that would have strongly supported β-barrel folding if vesicles had been present) and observed by fluorescence spectroscopy that U_{AQ} slowly self-associated on the time scale of hours.

We previously investigated the unfolded aqueous state (U_{AQ}) interactions of OmpA and 7 additional outer membrane proteins (OMPs) in buffers containing 1 M urea and found that OmpA was one of only a few OMPs to be entirely monomeric [24]. This result was contrary to the early findings of Surrey and Jähnig, but the urea concentration was higher in our experiments, and we reasoned that 1 M urea could completely destabilize OmpA oligomers [24]. Here we revisit this question of OmpA U_{AQ} self-association by measuring the protein concentration dependence of its sedimentation coefficient at lower concentrations of urea. Shown below, we did indeed observe self-interactions of OmpA unfolded states at urea concentrations more comparable to those used in the Surrey and Jähnig studies. Initially we controlled the set-up time for our sedimentation velocity (SV) experiments to be 30 minutes, in order to capture the physical parameters describing the "instantaneous" self-association that might compete with the productive folding of OmpA (when vesicles are present). However, we also show that self-association continues over the course of 12–16 hours, and we examined the concentration dependence of the rate of self-association (see below).

Primary sedimentation velocity data for $OmpA_{325}$ at 3 μM and in 450 mM urea are shown in Supplementary Fig. 2, where the separation between two boundaries is clearly evident. Fig. 4A shows the sedimentation coefficient distribution function obtained for the same dataset, using the time derivative method implemented in DCDT+ [22]. Under these conditions it can be observed that $OmpA_{325}$ is a mixture of a ~2 S species best described as monomer and a polydisperse ensemble of large oligomers with sedimentation coefficients in the range of 20–60 S. As described in Materials and methods, two separate analysis regions were used to obtain these distinct distributions. Fig. 4B shows similar results were obtained using the continuous $c(s^*)$ method in Sedfit [21]. In both cases, the monomer was so well separated from the oligomeric species, we could integrate the area under the two regions separately to determine the fraction monomer. Moreover, in all buffer conditions the ~2 S species is well described by a single Gaussian fit (implemented in DCDT+) that returns a molecular weight corresponding to the OmpA monomer. Integrating small and large *s*-value regions as well as confirming that the ~2 S region was monomeric OmpA was straightforward for all protein and urea concentrations.

Using sedimentation velocity, the fraction monomer was measured as a function of protein and urea concentrations for $OmpA_{325}$ and $OmpA_{171}$ at the 30 minute timepoint. These data are plotted in Fig. 5 and it can be observed that both proteins exhibit a sigmoidal dependence of self-association in three different urea concentrations: 300 mM (red), 450 mM (orange), and 600 mM (gold) urea. For both $OmpA_{325}$ and $OmpA_{171}$, low (<2) micromolar concentrations are required before the protein remains entirely monomeric for up to 30 minutes at these urea concentrations. Additionally, in all conditions $OmpA_{171}$ self-associates at lower total protein concentrations than the full-length $OmpA_{325}$ protein. The difference between these two proteins is the soluble periplasmic domain within $OmpA_{325}$, and these data therefore suggest that $OmpA_{Per}$ must act to reduce the propensity of $OmpA_{325}$ U_{AQ} to oligomerize.

The data are well described by the Hill equation, which gives the midpoint concentrations for fraction monomer. In Fig. 5C we show that the midpoint concentrations vary linearly with the urea concentration. By extrapolating to the absence of urea, we estimate the midpoint of $OmpA_{325}$ self-interaction to be ~200 nM, which means that very low protein concentrations should be required to avoid $OmpA_{325}$ oligomerization. Consistent with a more stable interaction, the $OmpA_{171}$ midpoint data extrapolates to a negative protein concentration, indicating that $OmpA_{171}$ self-association is always favorable. However, it should be noted that this linear extrapolation might flatten out at extremely low protein concentrations that we are not able to experimental access with the absorbance optics of the XL-A system. Nevertheless, oligomers of the OmpA barrel alone are clearly

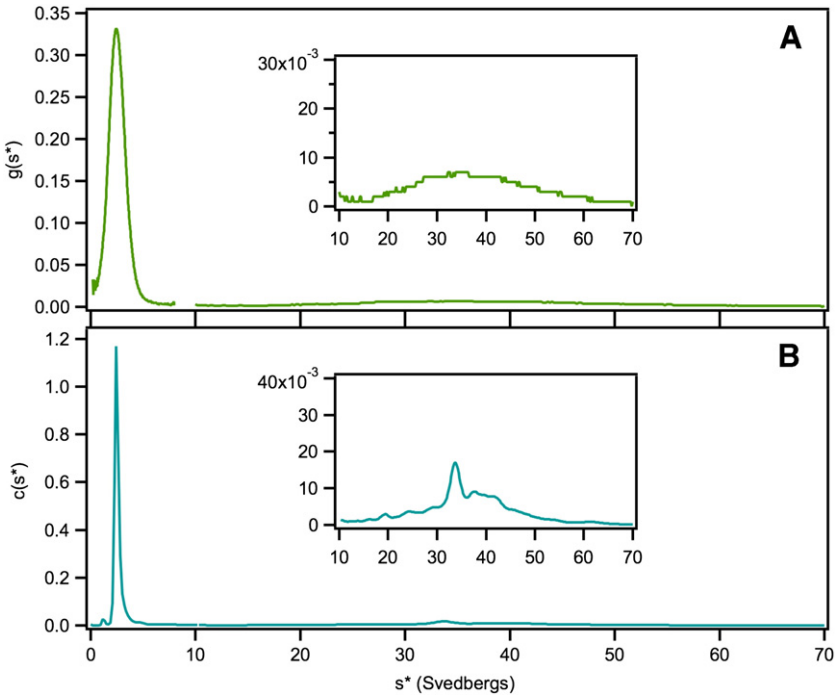

Fig. 4. Typical sedimentation velocity data analyzed by $g(s^*)$ and $c(s^*)$. Sedimentation velocity data are shown for 3 μM $OmpA_{325}$ in 450 mM urea, 2 mM TCEP, 20 mM Tris, pH 8. (A) Time derivative method of analysis as implemented in DCDT+. (B) Continuous $c(s^*)$ method of analysis as implemented in Sedfit. Inset panels show a zoom-in of the high s region. Integration of both curves gives 75% monomer (s-value 2.35).

more stable than the full-length protein, indicating that the periplasmic domain acts to disfavor self-association when covalently attached to the barrel domain (in cis).

To test whether the periplasmic domain is also able to influence OmpA self-association when not directly attached to the barrel domain (in trans), we performed sedimentation experiments with $OmpA_{Per}$ added separately to solutions of $OmpA_{325}$ or $OmpA_{171}$. One could imagine two indications of periplasmic domain–barrel interaction: a decrease in the fraction of oligomeric protein as measured by integration of the $g(s^*)$ curve, and the presence of a new peak in the $g(s^*)$ curve at an s-value consistent with the molecular weight of a complex. However, no significant change was observed in the fraction monomer at 30 minutes of either $OmpA_{325}$ or $OmpA_{171}$, with up to a four-fold molar excess of $OmpA_{Per}$ (data not shown). Additionally, we did not observe a complex peak in the small s-value region for these same mixtures. Supplementary Fig. 3 shows representative data for mixtures with a two-fold excess of $OmpA_{Per}$. We found that the $g(s^*)$ curve is well described by a calculated curve for a non-interacting mixture (simply a sum of the curves for the two proteins alone, scaled according to the concentrations in the mixture). Altogether these data show that the periplasmic domain does not form a stable complex with the unfolded barrel domain at these micromolar concentrations, and it must be covalently attached in order to reduce self-association of the barrel domain.

3.3. The unfolded OmpA β-barrel associates with a rate-limiting, critical nucleus size of 3 molecules

Fig. 5 shows a snapshot of OmpA self-association, as all of the data correspond to the fraction monomer present after only 30 minutes of incubation at low urea. We were also interested in determining the time-dependence of the self-association reaction and we utilized both sedimentation velocity and circular dichroism to monitor the extent of oligomerization over time. SV experiments were carried out for various total protein concentrations as described above, but with increasing incubation times, in order to sample different time points during the course of the reaction. The measured fraction monomer values at each time point for each concentration are shown as open circles in Fig. 6A and B for $OmpA_{325}$ and $OmpA_{171}$, respectively.

Overlaid upon the sedimentation velocity data points are the CD traces representing the signal decay of monomeric $OmpA_{325}$ and $OmpA_{171}$ (Fig. 6 panels A and B, respectively). The CD signal reflects the change in the secondary structure at 218 nm shown in the wavelength scan of Fig. 2D. We measured the kinetics of this CD signal change over the course of 15–17 hours for various OmpA concentrations. The curves were converted to fraction monomer and are plotted in Fig. 6 as solid lines for comparison with the SV data. For $OmpA_{171}$ (panel B), the time-dependent decrease in fraction monomer measured by CD agrees very well with the SV data, and it is evident that higher initial concentrations of protein lead to a more rapid decrease in monomer concentrations and a lower equilibrium value of fraction monomer. Both of these features are consistent with a self-association reaction. In contrast, the $OmpA_{325}$ CD curves do not agree with the SV data; the CD signal appears not to decay as fast as the fraction monomer time points measured by SV and therefore it would appear that the two techniques are not measuring the same physical process. One explanation for this observation is that the structural change that leads to a more negative CD signal is a separate process from the association into particles that sediment with high s-values. In the case of $OmpA_{171}$, which is composed of the barrel domain only, these processes apparently occur at the same rate. But for $OmpA_{325}$, which includes the soluble periplasmic domain, the change in secondary structure occurs more slowly than the association into faster-sedimenting particles.

To further investigate the nature of the $OmpA_{171}$ barrel self-association reaction, we used the method of initial rates to determine the order of the reaction (see Materials and methods) [8]. Fig. 7A shows a double logarithmic plot of the initial rates as a function of total protein concentration, determined from the $OmpA_{171}$ CD kinetics data. A linear fit to these data points gives a slope of 3.2, which corresponds to the order of the reaction. Therefore the rate-limiting step of self-association appears to involve the interaction of

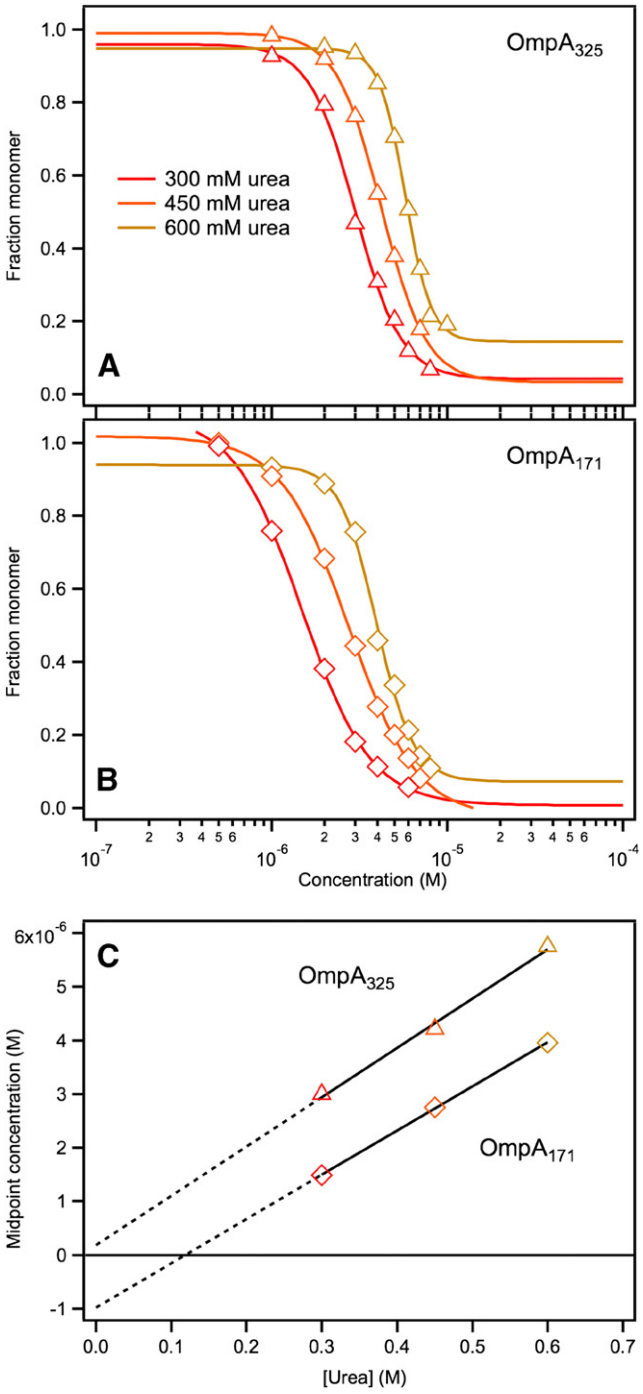

Fig. 5. OmpA self-association as a function of concentration and urea. Varying concentrations of $OmpA_{325}$ (A) and $OmpA_{171}$ (B) were prepared at 300 mM (red), 450 mM (orange), or 600 mM (gold) urea. Samples were incubated at 25 °C for 30 minutes before beginning centrifugation. Sedimentation velocity data were analyzed by the time derivative method and the $g(s^*)$ curves integrated to determine the fraction of monomeric protein at each concentration (open symbols). Solid lines show fits to the Hill equation. (C) The midpoints of the Hill fits are plotted as a function of urea, fitted to a line and extrapolated to the absence of urea. These intercepts are 0.2 μM and −1 μM for $OmpA_{325}$ and $OmpA_{171}$, respectively.

three $OmpA_{171}$ molecules. We attempted to fit the kinetic curves to the integrated rate equation for a third order reaction but this returned poor fits and varying values of rate constant (data not shown), suggesting the kinetics are more complex and may involve multiple kinetic phases, the elucidation of which are beyond the scope of this paper. However it is still evident that the initial rate-limiting step involves three $OmpA_{171}$ molecules.

Interestingly, we never observed intermediate-sized species by sedimentation velocity so we reasoned that the protein could be undergoing a nucleated growth polymerization reaction where the nucleus is not appreciably populated [20]. This type of reaction involves initial formation of an energetically unfavorable nucleus, followed by rapid elongation into polymer by the addition of monomer units. Analysis of the time-dependence of polymer formation allows determination of the critical nucleus size (n^*) necessary to facilitate downhill polymerization (see Materials and methods). In brief, the concentration of monomers incorporated into polymer should have a linear dependence on time squared at very early time points. A double logarithmic plot of these slopes as a function of total monomer concentration will also be linear, with a slope equal to n^*+2. The resulting values determined from the $OmpA_{171}$ CD kinetics data are shown in Fig. 7B and a linear fit to the data gives a slope of 4.6, or a critical nucleus of 2.6. Therefore ~3 OmpA molecules must condense to form a nucleus that then undergoes further oligomerization to form higher molecular weight species, which we observe in the large s-value region of our SV data. This alternative analysis is highly consistent with the order of reaction we determined to be three, so it is clear that OmpA self-association involves the initial formation of a nucleus of ~3 molecules before further association occurs.

3.4. OmpA self-association reduces folding efficiency when there is a delay in the addition of membranes

To determine the effect of oligomer formation on β-barrel folding, we conducted a delayed folding assay in which $OmpA_{325}$ and $OmpA_{171}$ were allowed to incubate for 30 minutes prior to the addition of $diC_{10}PC$ LUVs. If self-association of unfolded states competes with folding, we reasoned the folding of $OmpA_{171}$ should be reduced compared to $OmpA_{325}$ because it has a greater propensity for self-association. Fig. 8 shows the fraction folded of $OmpA_{325}$ (panel A) and $OmpA_{171}$ (panel B) at a total concentration of 2 μM or 5 μM in 600 mM urea, 20 mM Tris, pH 8. The first set of bars shows that both proteins at both concentrations fold with efficiencies close to 1 when there is no delay time (i.e. membranes are present when the protein is diluted into the folding mixture). When there is a 30-minute delay before the addition of vesicles, the second set of bars shows that the fraction folded is reduced to different extents. The $OmpA_{325}$ folding efficiency at 2 μM is reduced to 0.93 (±0.03) while folding efficiency at 5 μM is reduced to 0.72 (±0.03). These values correspond almost exactly to the fraction monomer measured under the same conditions by sedimentation velocity (shown in Fig. 5A). $OmpA_{171}$ folding efficiencies are reduced to 0.85 (±0.03) at 2 μM and 0.66 (±0.07) at 5 μM, which are also similar to the fraction monomer values measured by SV (Fig. 5B), and are consistently lower than the corresponding fraction folded for $OmpA_{325}$. Altogether these data indicate that OmpA barrel folding successfully competes against oligomerization when membranes are present from the time of dilution into low urea, but when given the time to self-associate, oligomeric unfolded protein is unable to dissociate and fold within 3 hours and thus there is a reduction in folding efficiency. We also failed to observe an effect on fraction folded when either $OmpA_{325}$ or $OmpA_{171}$ were incubated with equimolar concentrations of $OmpA_{Per}$ before the addition of vesicles, as shown by the third set of bars in Fig. 8. This result is consistent with the sedimentation velocity results described above, and further demonstrates that the periplasmic domain acts in cis but not in trans to affect OmpA self-association.

3.5. The folding competent unfolded conformations of $OmpA_{171}$ and $OmpA_{325}$ are expanded

The conformation of the unfolded state is the reference point for the development of kinetic folding models. Importantly, it is

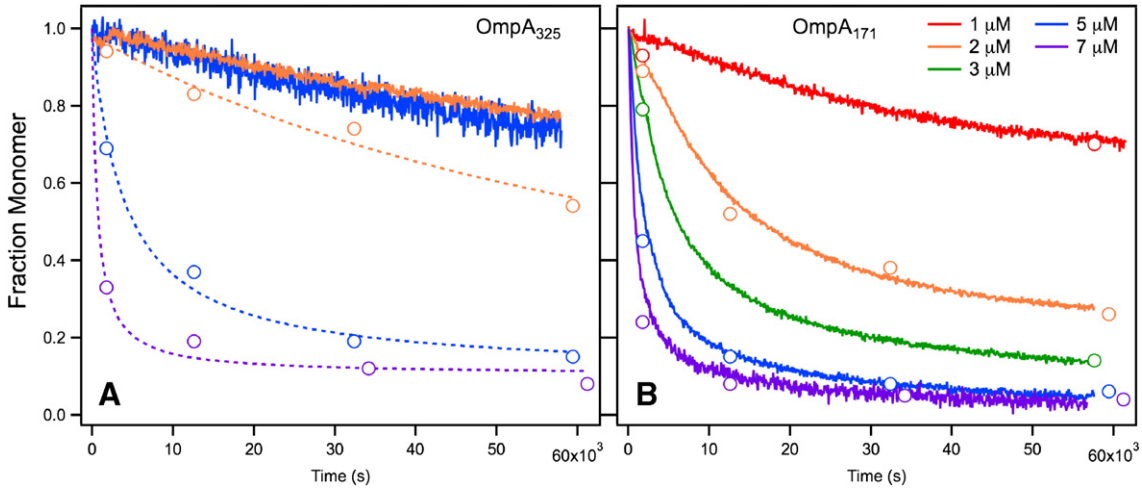

Fig. 6. Concentration dependence of self-association kinetics. Fraction monomer is plotted as a function of time for various total protein concentrations of $OmpA_{325}$ (A) and $OmpA_{171}$ (B). All samples were measured in 600 mM urea, 20 mM Tris, pH 8, and 25 °C. Open circles correspond to values measured by sedimentation velocity while solid lines show CD data converted to fraction monomer. Concentrations are denoted by color and are listed in the figure key. Dotted lines in (A) are shown only to guide the eye along the SV data.

the "folding competent" non-native state that would be populated under folding conditions that is the relevant conformation, not the conformation of the denatured state ensemble observed at

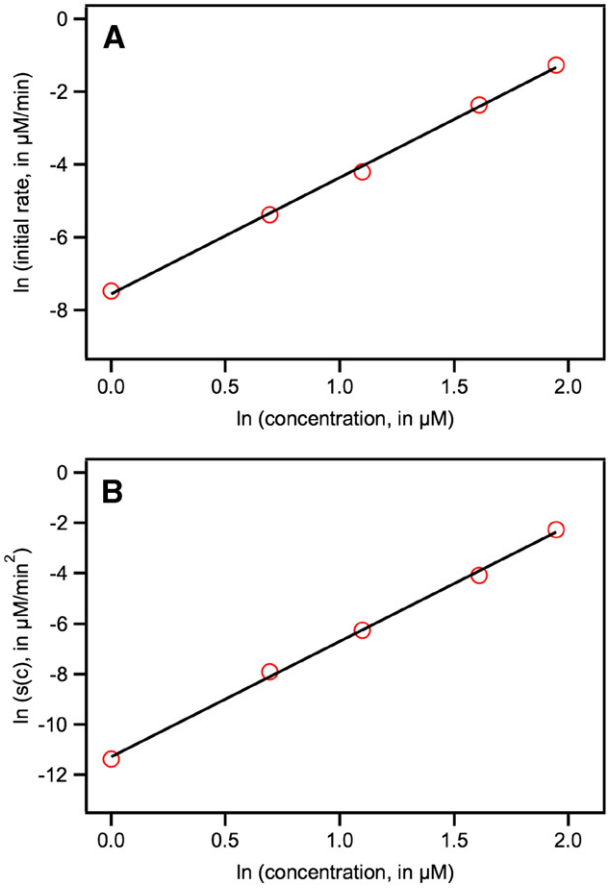

Fig. 7. Analysis of $OmpA_{171}$ CD kinetics. (A) Double logarithmic plot of initial rates of monomer disappearance as a function of initial monomer concentration. A linear fit of the data gives a slope of 3.2, which is interpreted as the order of the reaction. (B) Analysis of association kinetics by a nucleated growth polymerization model (see Materials and methods). The slope of the double logarithmic plot corresponds to n^*+2, where n^* is the critical nucleus size. This was found to be 4.6, giving a critical nucleus of 2.6 OmpA molecules.

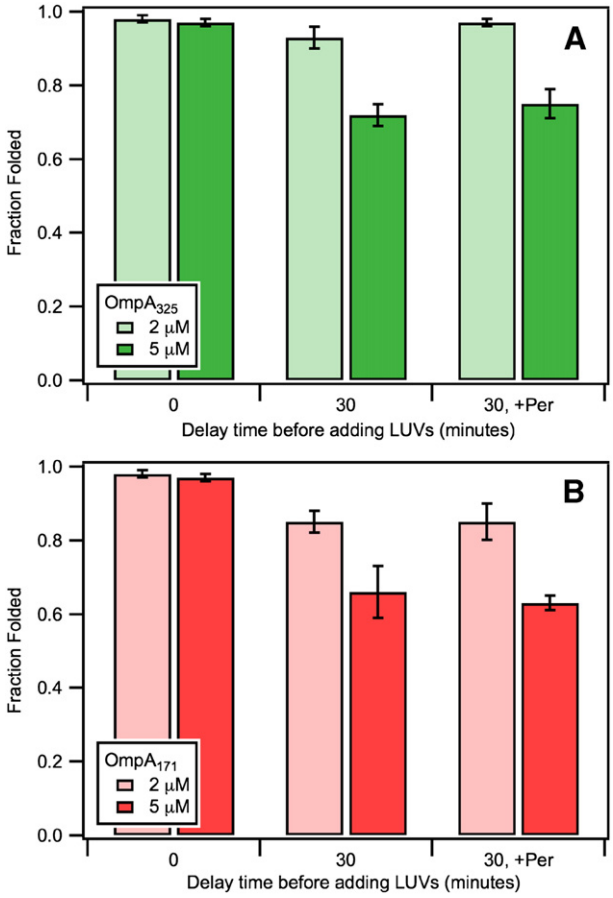

Fig. 8. Delayed folding of $OmpA_{325}$ and $OmpA_{171}$. Fraction folded is plotted for all samples after a delay of 0 or 30 minutes followed by folding for 3 h. Values are the average of 3–6 separate folding samples and error bars are the calculated standard deviation. $OmpA_{325}$ (A) and $OmpA_{171}$ (B) samples were prepared at 2 μM or 5 μM in 600 mM urea and incubated at 25 °C. After the appropriate delay, $diC_{10}PC$ LUVs were added at a final lipid to protein ratio of 800:1 and folding was allowed to occur for 3 h with gentle stirring before quenching by the addition of 5× SDS-PAGE loading buffer to a final concentration of 1×. Fraction folded was determined by densitometry of folded and unfolded bands. Data labeled "+Per" indicate samples incubated during the 30 minute delay with equimolar concentrations of $OmpA_{Per}$ (2 μM or 5 μM).

high (>6 M) urea concentrations. Since membrane proteins require phospholipid vesicles to fold, we are uniquely suited to populate the relevant unfolded state by simply leaving out vesicles from the reaction. Because U_{AQ} states self-associate so strongly (shown above), we cannot directly visualize monomeric unfolded states in the absence of urea. However, we are able to tune the urea concentration to populate monomer and determine the sedimentation coefficient as a function of urea. At 2 μM total protein, we found that the sedimentation coefficients are a linear function of urea concentration, which means we can extrapolate the values to the absence of denaturant. These data are shown in Fig. 9, and the $s^*_{20,w}$ values for $OmpA_{325}$ and $OmpA_{171}$ extrapolate to 2.34 S and 1.65 S, respectively. These values correspond to f/f_o values of 1.68 and 1.60, respectively. We used Sednterp to interpret these data in terms of the simple molecular envelope of a prolate ellipsoid of revolution. Our results suggest expanded conformations for both of these proteins, with axial ratios of 8.3:1 and 7.3:1, respectively for $OmpA_{325}$ and $OmpA_{171}$.

4. Discussion

4.1. Unfolded conformations as a reference point for kinetic folding models

Despite the extensive studies on OmpA folding, there are still kinetic phases and conformations that are not well understood. In particular, the self-association propensity of aqueous, unfolded OmpA has not previously been extensively investigated. We find that both the $OmpA_{171}$ barrel and the full-length $OmpA_{325}$ protein show significant propensities to form very large oligomeric structures when there is a delay in the addition of lipids. As previously shown for OmpT [24], the weight average sedimentation coefficients of OmpA are in the 20–60 S range, comparable to the size of ribosomal subunits. In contrast, we expect that the thermodynamic stabilities of these OmpA oligomers must be less than the stabilities for OmpT U_{AQ} oligomers, as it requires much lower concentrations of urea to melt OmpA oligomers into monomers as compared to the previous studies on OmpT.

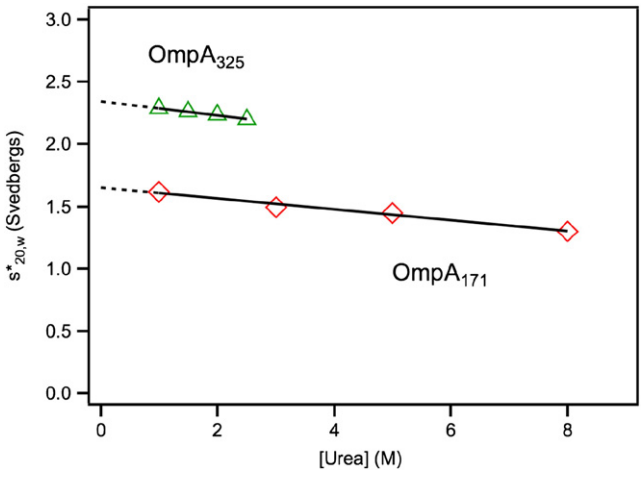

Fig. 9. Sedimentation coefficients extrapolated to the absence of urea. $s^*_{20,w}$ values from single-species fits of $g(s^*)$ curves for $OmpA_{325}$ and $OmpA_{171}$ are plotted as a function of urea concentration. $OmpA_{171}$ (red diamonds) was studied in urea concentrations ranging from 1 M to 8 M. $OmpA_{325}$ (green triangles) was studied in urea concentrations of 1 M to 2.5 M, in order to measure the sedimentation coefficient in the region below the unfolding transition of the periplasmic domain. The data were fit to linear functions and the sedimentation coefficients extrapolated to a urea concentration of zero. These values were found to be 2.34 S for $OmpA_{325}$ and 1.65 S for $OmpA_{171}$.

We have further shown that the unfolded conformation of the OmpA barrel shows no regular structure. The interpretation of our CD data is in contrast to early studies implying that membrane-embedded regions of U_{AQ} OmpA possessed a mixed alpha/beta secondary structure in aqueous solution. Rather, these secondary structure features of OmpA arise from folding of its soluble periplasmic domain, which is stable independent of the OmpA transmembrane β-barrel. The "folding competent" non-native state also has a CD signature quite distinct from that of the OmpA oligomers that form at higher concentrations over the time period of 12–16 hours; the latter state has a very broad negative peak in the beta region of the CD spectrum and lacks the 231 nm peak found in the native OmpA β-barrel. Since these oligomers form slowly and are of such high molecular weight, it is interesting to speculate that these are crossed-beta structures reminiscent of the types that amyloidal proteins can form. However, future experimentation using more specific structural and/or dye binding assays need to be carried out to test this hypothesis.

A third aspect of the OmpA unfolded conformation that we investigated relates to its level of compactness. It had previously been proposed that $OmpA_{325}$ forms a collapsed aqueous state that then folds into membranes [4,8]. However, this concept raises the question of how this conformation can then "uncollapse" to be able to partition onto membrane surfaces in a folding-competent state. Our sedimentation velocity data show, in fact, that the monomeric U_{AQ} forms of both $OmpA_{325}$ and $OmpA_{171}$ adopt expanded conformations. This starting point for folding rationalizes the need for these proteins to effectively partition onto membranes in a productive structure.

4.2. Competition between U_{AQ} self-association and folding kinetics

Another aspect of the *in vitro* folding pathway that remains to be investigated is the thermodynamic potential for partitioning of U_{AQ} states onto the membrane surface. Certainly the data show that this reaction competes quite effectively because the proteins do fold. Therefore, the consequences of U_{AQ} self-association will strongly depend on how quickly the proteins partition onto membranes and whether or not all membrane binding occurs in folding-competent conformations. Even if some membrane binding conformations are not productive for folding, membrane binding will reduce the total aqueous OmpA concentration, which should diminish oligomer formation. Moreover, early kinetic events that may be affected by U_{AQ} self-association will be essential to investigate in a systematic manner. Already, we observed that the rate of $OmpA_{325}$ self-association occurs faster than the secondary structure change that is ultimately indicative of the large oligomer formation. Multiple orthogonal methods must be applied to fully dissect the kinetic details of these two processes. While we did not observe any loss of folding *efficiency* over a 3-hour period if membranes were immediately available to U_{AQ} $OmpA_{325}$ and $OmpA_{171}$, our data do not exclude an effect on folding *kinetics*. It could be that U_{AQ} oligomers slow the folding of both $OmpA_{325}$ and $OmpA_{171}$. A future comparison of folding rate constants will be necessary to address these questions.

4.3. The OmpA periplasmic domain possesses chaperone activity when covalently attached to the OmpA β-barrel

Since both $OmpA_{325}$ and $OmpA_{171}$ can fold *in vitro* upon the addition of synthetic phospholipid vesicles, it is obvious that their sequences contain all the molecular information needed to fold these proteins into their native conformations [14,25]. However, along with other OMPs, OmpA needs to remain in a folding-competent state in the cell until it is sorted to the outer membrane in bacteria. Elaborate cellular machinery exists to ensure proper membrane

compartmentalization of these proteins [26]. It is clear from the work in this study that self-association of the OmpA unfolded state represents a reaction that competes with folding. Although there is no loss in folding efficiency when membranes are present from the time of dilution to low urea, there is a decrease in folding when the proteins are incubated at low urea and self-association is allowed to occur before the addition of membranes. Indeed in the cell the proteins encounter an environment more like the second situation since they must traverse the aqueous periplasm in the unfolded state before encountering the outer membrane. Self-association *in vitro* competes with folding even when folding is allowed to proceed for 3 hours, which is already a time period much longer than the doubling time of *E. coli*. Therefore the prevention of self-association while the unfolded OMPs proceed to the outer membrane is probably a major role for periplasmic chaperones.

In this study we discovered a novel chaperone function of the periplasmic domain of OmpA whereby it can act to increase folding efficiency by reducing self-association when present in cis (i.e. as part of $OmpA_{325}$). However, $OmpA_{Per}$ is unable to reduce self-association when added separately to the barrel domain. We observed neither an increase in fraction monomer nor any indication of a stable complex formed between OmpA's β-barrel and periplasmic domains when $OmpA_{Per}$ is added in micromolar concentrations. Therefore the interaction between $OmpA_{Per}$ and the OmpA barrel domain must be a relatively weak one. Nevertheless, the periplasmic domain does have an effect within the full-length protein: $OmpA_{325}$ —with the periplasmic domain covalently attached—self-associates less and displays less of a loss in folding efficiency upon incubation without vesicles. There may also be an effect on the thermodynamic stability of the protein because Sanchez et al. proposed that the soluble periplasmic domain might stabilize an unfolded conformation of the OmpA β-barrel [25].

Even though the full-length $OmpA_{325}$ self-associates less than just the transmembrane β-barrel alone, both proteins form large oligomeric species at micromolar concentrations in low concentrations of urea. Therefore, we speculate that additional cellular factors must be involved in preventing OmpA self-interactions *in vivo*. Extrapolated to the absence of urea, the midpoint of oligomer formation of full-length OmpA is ~200 nM, which means that such assembly factors must bind with nanomolar affinities in order to thermodynamically compete with oligomerization. A likely candidate is the Skp_T protein, which has been shown to stoichiometrically bind to a number of outer membrane proteins at sub-micromolar concentrations, including OmpA [27,28]. The cell therefore uses significant free energy to sequester OmpA into a Skp_T:OmpA complex. The data presented here on OmpA U_{AQ} self-interactions rationalize why the free energy of Skp_T binding needs to be so favorable.

Supplementary materials related to this article can be found online at doi:10.1016/j.bpc.2011.06.013.

Acknowledgements

This work was supported by grants from the NSF (MCB 0919868) and the NIH (R01 GM079440 and T32 GM008403). EJD is a recipient of an NSF graduate research fellowship (DGE-0707427). We thank Professor Blake Hill for the TEV expression plasmid and Mr. Michael Genualdi for cloning and purifying $OmpA_{Per}$.

References

[1] N.A. Rodionova, S.A. Tatulian, T. Surrey, F. Jähnig, L.K. Tamm, Characterization of two membrane-bound forms of OmpA, Biochemistry 34 (1995) 1921–1929.
[2] L.K. Tamm, H. Hong, B. Liang, Folding and assembly of beta-barrel membrane proteins, Biochim. Biophys. Acta 1666 (2004) 250–263.
[3] J.H. Kleinschmidt, L.K. Tamm, Folding intermediates of a beta-barrel membrane protein. Kinetic evidence for a multi-step membrane insertion mechanism, Biochemistry 35 (1996) 12993–13000.
[4] T. Surrey, F. Jähnig, Kinetics of folding and membrane insertion of a beta-barrel membrane protein, J. Biol. Chem. 270 (1995) 28199–28203.
[5] R. Freudl, H. Schwarz, Y.D. Stierhof, K. Gamon, I. Hindennach, U. Henning, An outer membrane protein (OmpA) of *Escherichia coli* K-12 undergoes a conformational change during export, J. Biol. Chem. 261 (1986) 11355–11361.
[6] J.H. Kleinschmidt, M.C. Wiener, L.K. Tamm, Outer membrane protein A of *E. coli* folds into detergent micelles, but not in the presence of monomeric detergent, Protein Sci. 8 (1999) 2065–2071.
[7] K. Dornmair, H. Kiefer, F. Jähnig, Refolding of an integral membrane protein. OmpA of *Escherichia coli*, J. Biol. Chem. 265 (1990) 18907–18911.
[8] J.H. Kleinschmidt, L.K. Tamm, Secondary and tertiary structure formation of the beta-barrel membrane protein OmpA is synchronized and depends on membrane thickness, J. Mol. Biol. 324 (2002) 319–330.
[9] H. Hong, L.K. Tamm, Elastic coupling of integral membrane protein stability to lipid bilayer forces, Proc. Natl. Acad. Sci. U. S. A. 101 (2004) 4065–4070.
[10] A. Pautsch, G.E. Schulz, High-resolution structure of the OmpA membrane domain, J. Mol. Biol. 298 (2000) 273–282.
[11] H. Hong, S. Park, R.H. Jimenez, D. Rinehart, L.K. Tamm, Role of aromatic side chains in the folding and thermodynamic stability of integral membrane proteins, J. Am. Chem. Soc. 129 (2007) 8320–8327.
[12] H. Hong, G. Szabo, L.K. Tamm, Electrostatic couplings in OmpA ion-channel gating suggest a mechanism for pore opening, Nat. Chem. Biol. 2 (2006) 627–635.
[13] T. Surrey, F. Jähnig, Refolding and oriented insertion of a membrane protein into a lipid bilayer, Proc. Natl. Acad. Sci. U. S. A. 89 (1992) 7457–7461.
[14] N.K. Burgess, T.P. Dao, A.M. Stanley, K.G. Fleming, Beta-barrel proteins that reside in the *Escherichia coli* outer membrane in vivo demonstrate varied folding behavior in vitro, J. Biol. Chem. 283 (2008) 26748–26758.
[15] S. Grizot, S.K. Buchanan, Structure of the OmpA-like domain of RmpM from *Neisseria meningitidis*, Mol. Microbiol. 51 (2004) 1027–1037.
[16] T.M. Laue, B.D. Shah, T.M. Ridgeway, S.L. Pelletier, Computer-aided interpretation of analytical sedimentation data for proteins, in: S. Harding, A. Rowe, J. Hoarton (Eds.), Analytical Ultracentrifugation in Biochemistry and Polymer Science, Royal Society of Chemistry, Cambridge, UK, 1992, p. 90.
[17] R.B. Kapust, J. Tozser, J.D. Fox, D.E. Anderson, S. Cherry, T.D. Copeland, D.S. Waugh, Tobacco etch virus protease: mechanism of autolysis and rational design of stable mutants with wild-type catalytic proficiency, Protein Eng. 14 (2001) 993–1000.
[18] M.M. Santoro, D.W. Bolen, Unfolding free energy changes determined by the linear extrapolation method. 1. Unfolding of phenylmethanesulfonyl alpha-chymotrypsin using different denaturants, Biochemistry 27 (1988) 8063–8068.
[19] M.M. Santoro, D.W. Bolen, A test of the linear extrapolation of unfolding free energy changes over an extended denaturant concentration range, Biochemistry 31 (1992) 4901–4907.
[20] S. Chen, F.A. Ferrone, R. Wetzel, Huntington's disease age-of-onset linked to polyglutamine aggregation nucleation, Proc. Natl. Acad. Sci. U. S. A. 99 (2002) 11884–11889.
[21] P. Schuck, Size-distribution analysis of macromolecules by sedimentation velocity ultracentrifugation and lamm equation modeling, Biophys. J. 78 (2000) 1606–1619.
[22] J.S. Philo, Improved methods for fitting sedimentation coefficient distributions derived by time-derivative techniques, Anal. Biochem. 354 (2006) 238–246.
[23] M.A. Khan, C. Neale, C. Michaux, R. Pomes, G.G. Prive, R.W. Woody, R.E. Bishop, Gauging a hydrocarbon ruler by an intrinsic exciton probe, Biochemistry 46 (2007) 4565–4579.
[24] A. Ebie Tan, N.K. Burgess, D.S. DeAndrade, J.D. Marold, K.G. Fleming, Self-association of unfolded outer membrane proteins, Macromol. Biosci. 10 (2010) 763–767.
[25] K.M. Sanchez, J.E. Gable, D.E. Schlamadinger, J.E. Kim, Effects of tryptophan microenvironment, soluble domain, and vesicle size on the thermodynamics of membrane protein folding: lessons from the transmembrane protein OmpA, Biochemistry 47 (2008) 12844–12852.
[26] J.G. Sklar, T. Wu, D. Kahne, T.J. Silhavy, Defining the roles of the periplasmic chaperones SurA, Skp, and DegP in *Escherichia coli*, Genes Dev. 21 (2007) 2473–2484.
[27] P.V. Bulieris, S. Behrens, O. Holst, J.H. Kleinschmidt, Folding and insertion of the outer membrane protein OmpA is assisted by the chaperone Skp and by lipopolysaccharide, J. Biol. Chem. 278 (2003) 9092–9099.
[28] T.A. Walton, C.M. Sandoval, C.A. Fowler, A. Pardi, M.C. Sousa, The cavity-chaperone Skp protects its substrate from aggregation but allows independent folding of substrate domains, Proc. Natl. Acad. Sci. U. S. A. 106 (2009) 1772–1777.